POAC'15
Trondheim, Norway

Proceedings of the 23rd International Conference on
Port and Ocean Engineering under Arctic Conditions
June 14-18, 2015
Trondheim, Norway

CONFINED COMPRESSION TESTS ON SALINE AND FRESH FREEZE-BONDS

Ida Mari Bueide[1,2,3] and Knut Vilhelm Høyland[2]

[1]Multiconsult AS
[2]Sustainable Arctic and Marine and Coastal Technology (SAMCoT), Center for Research-based Innovation (CRI), Norwegian University of Science and Technology, Trondheim, Norway
[3]The University Center on Svalbard (UNIS)

ABSTRACT

Tri-axial compression tests were conducted on freeze-bonds in saline and fresh ice, with the objective to study the internal freeze-bond stresses in relation to increased radial confinement, as well as how to best conduct these experiments. Cylindrical samples with a freeze-bond at 45° were applied radial static confinement and vertical compression at a constant velocity. The chosen variables consisted of confinement, submersion time, initial temperature and salinity. A larger part of the configurations gave increasing freeze-bond stresses for increasing confinement, both when studying the peak and residual stress plots. Mohr-Coulombs failure criterion was applied and the peak stress plots gave estimated cohesion values in the range 0.003 – 0.099 MPa and 16 – 45° (0.28 - 0.78rad) for internal friction. For the residual stresses the cohesion values were approaching zero and internal friction angles were in the range 11 – 37° (0.19 - 0.65rad). In relation to initial temperature the lowest initial temperature of -8.5°C gave the highest cohesion values. And the configurations with fresh samples had a mean cohesion value 30 % higher than for saline.

INTRODUCTION

Developing a material model for an ice ridge is a long term process. The calculation of forces from ice ridges involves both the consolidated layer and the ice rubble. The ice rubble strength derives from the freeze-bonding and interlocking of ice blocks. Experimental investigations on freeze-bonds have been conducted both in the field and the larger part in the laboratory. Most investigations are done on the topic of freeze-bond strength and the parameters influencing it. Helgøy et al. (2013) recently published articles concerning freeze-bond strength and Repetto-Llamazares and Høyland (2011) compared previous articles results on freeze-bond strengths. Figure 1 shows a principle sketch of test set-ups applied in previous tests.

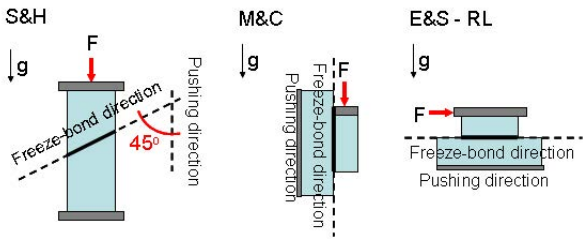

Figure 1. Illustration of experimental set-up from Repetto-Llamazares et al. (2011). S&H- Shafrova and Høyland (2008), M&C- Marchenco and Chenot (2009), E&S- Ettema and Shaefer (1986), RL- Repetto-Llamazares et al. (2011a)

Tri-axial compression tests were conducted on freeze-bonds in saline and fresh ice, with the objective to study the internal freeze-bond stresses in relation to increased radial confinement. Previously this dependency has been investigated by applying loads parallel to the freeze-bond, on top of ice blocks frozen together, as shown in Figure 1 (E&S - RL). A linear increase with increasing confinement has been observed for these experiments and a Mohr-Coulomb failure criterion has been suggested to describe the material. The experiments presented in this paper were conducted in order to investigate this further and to give estimated values of cohesion and internal friction to describe the material strength. The sample dimensions were determined by the devices used. The height of the sample of 150 mm was forced by the dimensions of the pressure clock and the diameter of 70 mm was given by the core sampler kovacs.

EXPERIMENTAL SET-UP

Tri-axial testing was conducted on cylindrical samples with a freeze-bond at 45°, by applying radial static confinement σ_r and vertical compression at a constant velocity. A principal sketch is presented in Figure 2.

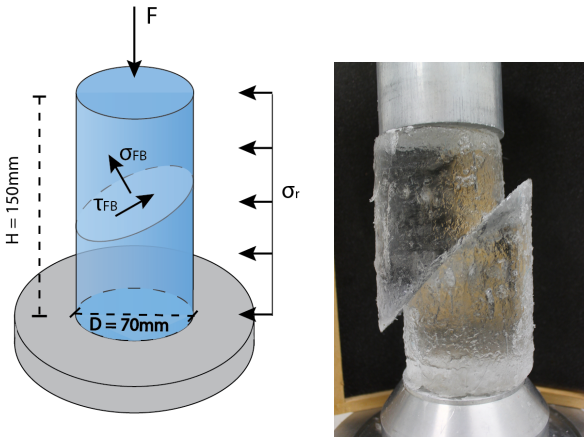

(a) (b)

Figure 2. a) Illustration of experimental set-up b) sample after testing

To prepare for the compression test, pre-cut samples were placed in the Cold-Lab until the ice was in thermal equilibrium with the air temperature, which was set to the desired initial temperature (T_i). The basin used to submerge the samples was also placed in the lab and continuously stirred until the desired temperature (T_w) was reached. The submersion water was set according to the freezing point of the water, -0.5°C for 8ppt and 0.0°C for the fresh water samples.

Firstly the dimensions of the sample was measured and logged before a 45° section was cut with a circular saw. Secondly the sample was assembled in a device called FIXIS, which holds the two cylindrical ice blocks together in a fixed position. This was then immediately submerged for a given time (Δt). The samples were submerged without any confinement. The salinity (S_w) and the temperature (T_w) of the submersion water were measured between each sample. After submersion the sample was removed from the FIXIS and placed in the pressure clock, which was then placed in the compression device. The pressure in the clock was set to the desired confinement value (σ_r) before the piston force was applied with a constant velocity (V).

The deformation limit was constrained by the height of the pressure clock, this sets the limit to 17-20 mm. Deformation (δh) and piston force was logged. After the tests the temperature of the sample ($T_{ice,test}$) was measured, the failure mode was recorded by observation together with relevant comments and pictures were taken. The sample was placed in a container to melt and later the salinity was measured.

Both fresh and saline ice was used in these tests. The fresh ice was collected from Isdammen in Longyearbyen over a period of time. By thin-sections it was defined as an S1 type with average grain size of 9 mm. The density varied between 920kg/m^3 and 941kg/m^3 depending on the air content. This is high, the maximum pure ice density is 917 kg/m^3. The saline samples were produced in the ice production basin FRYSIS at UNIS. A method of seeding as described by Helgøy et al. (2013) was used. The ice was defined as in-between S1 and S3 type and had a salinity of 2.2 - 2.8 ppt.

Test configurations

Four test series were conducted, two with fresh water samples submerged in fresh water and two with saline samples submerged in saline water (figure **??**). Each test series were divided into six configurations, where all were tested with three confinement values σ_r (equation 1). One exemption was made for the fresh water samples with initial temperature of -2.5°C, they were only tested for the two shortest submersion times because of weak freeze-bonds beyond this point.

$$\sigma_r = [0.0070 - 0.0094, 0.0200 - 0.0212, 0.0987 - 0.1026]MPa \quad (1)$$

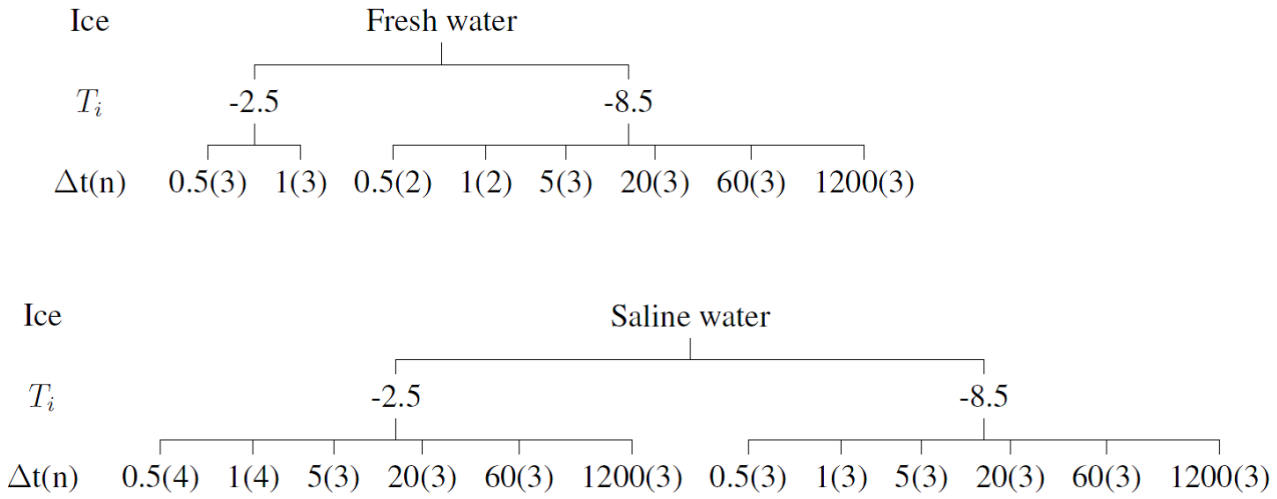

Illustration of test configurations. Ice temperature (T_i), submersion time (Δt) and number of samples (n) tested for each configuration

Force, stresses and velocity

The strength measurements were conducted in the compression machine KNEKKIS applying a vertical force at a constant velocity of 0.8 mm/s corresponding to a sliding velocity of 1.13 mm/s. The radial pressure was obtained by using a pressure clock. With a 45° compression angle relative to the freeze-bond a shear fracture resulting from displacement along this plane was obtained. The output data was an approximately static radial pressure and a time dependent force logged with a time step of 0.1 seconds. The piston force σ_z was defined as the logged force F divided by the circular area of the sample as shown in equation 2. The residual force was defined as the measured force after the peak was reached, divided by the circular area of the sample.

$$\sigma_z = \frac{Measuredpistonforce}{\pi r^2} \tag{2}$$

The peak and residual freeze-bond shear stress was calculated as shown in the appendix. The resulting freeze-bond stresses are shown in equation (3).

$$\begin{aligned} \sigma_{FB} &= \frac{8}{\pi^2}\sigma_r + \sigma_z - \sigma_{FB} \\ &= \frac{4}{\pi^2}\sigma_r + \frac{1}{2}\sigma_z \end{aligned}$$

$$\begin{aligned} \tau_{FB} &= \sigma_z - \frac{4}{\pi^2}\sigma_r - \frac{1}{2}\sigma_z \\ &= \frac{1}{2}\sigma_z - \frac{4}{\pi^2}\sigma_r \end{aligned} \tag{3}$$

These results were used to determine the peak stress dependency for the different parameters, and further to estimate cohesion values and internal friction angles.

PEAK SHEAR STRESS

Results

In Figure 3 the freeze-bond stress τ_{FB} was plotted according to submersion time Δt, the saline experiments in Figure 3 a) and the fresh in 3 b). We found a bell-curve development of the stress vs submersion time, as suggested by Shafrova and Høyland (2008) and found experimentally Repetto-Llamazares et al. (2011). The fresh water samples generally peaked at shorter submersion times than the saline. For the initial temperature of -8.5°C the curve peaked at submersion times of 5 min or less, while for the initial temperature of -2.5°C the curve peaked at submersion times of 1 min or less. For both saline and fresh water samples the peak shear stress increased with decreasing initial temperature.

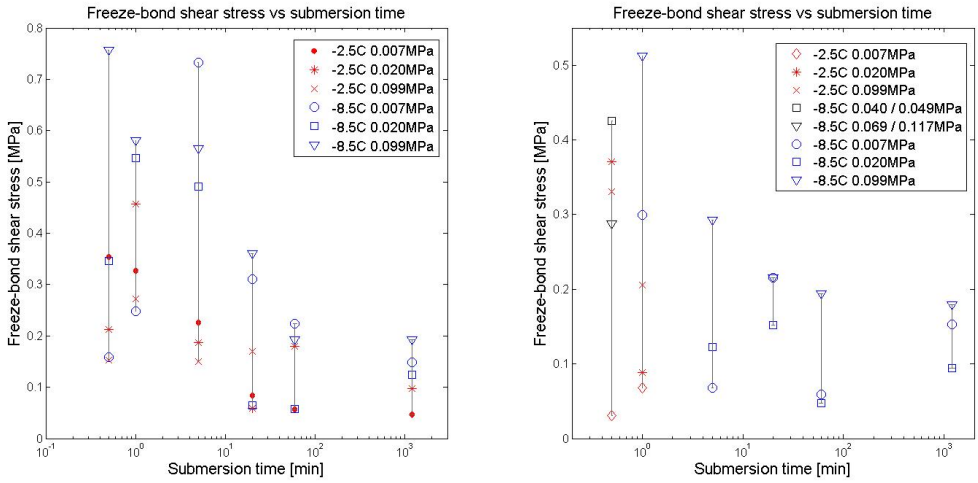

(a) (b)

Figure 3. Submersion time Δt vs freeze-bond shear stress τ_{FB}. a) saline water experiments b) fresh water experiments

In Figure 4 all salinities are displayed depending on submersion time. The salinity at 0.5 and 1 min was found to be stable at the level before submersion. For 5 - 60 min submersion times the salinity had a large variation between each sample. Samples submerged longer than 60 min had a clearly reduced salinity. The samples with initial temperature of -2.5°C generally had the lowest salinities.

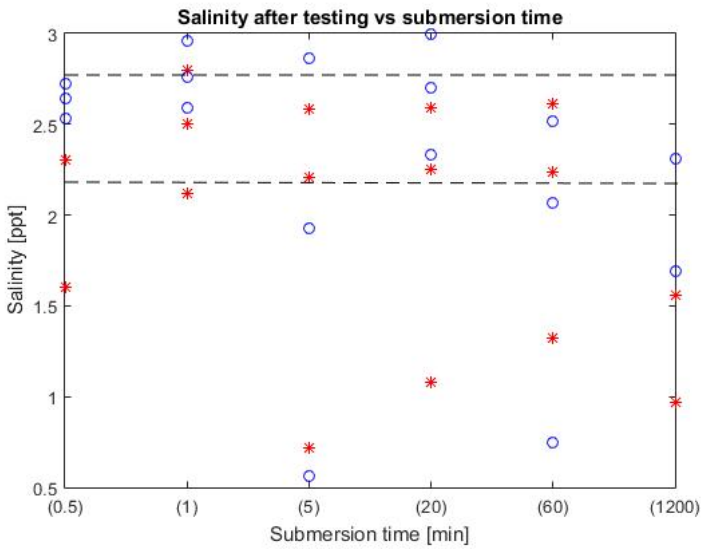

Figure 4. Salinity for all saline samples after testing sorted by submersion time. The red stars indicate initial temperature of -2.5°C and the blue circles -8.5°C. Span of initial salinity indicated by dotted lines.

Discussion

A bell-curve development of the stress described the stress dependency on submersion time. The fresh water samples generally peaked at shorter submersion times. A lower porosity in these samples increases the thermal conductivity. Air filled pockets also have a higher mass diffusion than brine filled pockets. This suggests that the potential energy will be transferred at a higher rate for fresh ice, causing the strength to peak at an earlier time. This trend agrees with the predictions of Shafrova and Høyland (2008), and the suggested driving forces, temperature and salinity, can be distinguished by that the fresh samples had a quicker first phase and a similar second and third phase development. The phases were described by Repetto-Llamazares et al. (2011).

The fresh water samples at -2.5°C were only strong enough to be tested for the shortest submersion times. The reduction in strength occurs quickly after reaching the peak strength. Why the strength did not stabilize as for saline samples and for the lower initial temperature remains unanswered.

The shear stress was higher for the lowest initial temperature, for both fresh and saline water. Shafrova and Høyland (2008) (initial temperatures from -1.8°C to -7.2°C) found the same trend for submerged fresh water samples, while Repetto-Llamazares et al. (2011) observed the opposite, increasing stress with increasing initial temperature as a clear trend, but only for the lowest confinement. Høyland and Møllegaard (2014) found that the stress was highest for the initial temperature of -8.5°C and lower for both -15°C and -2.5°C. The initial temperature has two effects on the freeze-bond stress. Firstly a lower initial temperature implicates that it takes longer before the sample reaches equilibrium with the submersion water, meaning it may be colder than the water during testing. This also affects

the brine content, faster ice growth locks in more brine. Secondly the speed of which the freeze-bonds form is higher. The strongest ice may be found at intermediate temperatures as suggested by Høyland and Møllegaard (2014).

The temperature development in the ice varied for the two initial temperatures. The samples at -2.5°C had a stable temperature for the submersion times of 0.5 and 1 min, before it started to increase. The samples at -8.5°C had increasing temperature from the shortest submersion time. The higher temperature gradient may explain the faster change. For both the temperatures the samples reached equilibrium with the water between 60 and 1200 min.

The saline samples increased in size during submersion while the fresh samples decreased. A redistribution of energy in the saline sample during warming, melting of ice in the sample releases energy which causes ice to form on the outside of the sample, explains this observation (Shestov and Marchenko, 2013). The salinity was measured both before and after testing. The salinity of the fresh water samples increased to that of the submersion water, which was still very low. For the saline samples the salinity decreased during submersion. This was assumed to result from brine drainage over time. This agrees with what was found by Møllegaard (2012), he measured the salinity of the freeze-bond specifically and found that it varied in the plane, more drainage towards the edges. In our experiments the freeze-bond section amounted to a relatively small area, making the drainage of brine a visible effect. For the intermediate submersion times of 5 - 20 min there were large variations in the salinity, this could indicate that drainage was on-going at this stage and reached equilibrium after 60 min.

The lowest salinities were measured for the highest initial temperature of -2.5°C for most samples. Likely this was due to the establish fact that faster ice growth locks in more brine. A lower salinity gives higher freeze-bond strength, but at the same time the lower temperature gives a higher strength. In general the samples with the lowest initial temperature had the highest freeze-bond strength. The initial temperature has a stronger influence on the peak stress than the salinity in these experiments.

Møllegaard (2012) found the peak stresses to be in a higher range than we found in this study. He used a similar test set-up, but the sample was longer (by 25 mm). We compared uni-axial samples at the two different heights it was found that the shorter sample gave lower freeze-bond stress. Shafrova and Høyland (2008) found peak stresses in the upper range for the uni-axial laboratory test. Ettema and Schaefer (1986), Repetto-Llamazares et al. (2011) Ettema and Shafer (1986) and Helgøy et al. (2013) studied the peak stress using direct shear tests. Their results were in the range 0.006 - 0.030 MPa, much lower than the tests with 45° set-up angle. This may be explained by an analysis in the τ-σ-plane, comparisons of the estimated cohesion and internal friction angle are presented in the next section.

THE τ-σ PLANE AND THE DERIVATION OF COHESION AND INTERNAL FRICTION VALUES

Results

The shear stress – confinement developments were studied. To describe the different developments 5 types were defined as listed below. The small sample basis limits the failure slope to be linear. With more samples the failure slope could show that a non-linear development would be appropriate. A least squares approach was used to estimate the failure slope.

1. Increasing shear stress with increasing confinement
2. Increasing shear stress with increasing confinement up to 0.020 MPa
3. Intermediate stress for the lowest confinement, lowest stress for the intermediate confinement and highest stress for the highest confinement
4. Highest stress for the lowest confinement, lowest stress for the intermediate confinement and intermediate stress for the highest confinement
5. Decreasing stress with increasing confinement

Most configurations were defined as type 1), these are the configurations used for calculating cohesions and internal friction angles. 6 out of 20 peak shear stress configurations and 14 out of 20 residual shear stress configurations had this development. The residual shear stress – confinement developments were more often defined as type 1), independent of the appertaining development type found for the peak stress.

The configurations in the 4 other categories may arise from premature failure. Three possible interpretations were considered. The first, a weakness in the sample, due to handling during testing or production. The second, a softening of the material. And the last that the radial confinement exceeded the strength of the freeze-bond, and it had already failed when the vertical compression was applied, this was observed only for the highest radial confinement. During testing when the radial force was applied we could hear the sample failing.

The interpretation of softening was looked into by estimating failure slopes from two samples and extrapolating it too the third sample. A line was fitted through the failure points of the samples with the two highest or the two lowest confinements. Assuming the first line to give an approximately correct tensile stress, this was used as a starting point for the second failure slope. If this assumption was suitable is unknown. The maximum difference in cohesion for the fitted and extrapolated line was 0.0054 MPa, which was in the order of 26.6 % lower. The internal friction angle was also in the same order less.

The third interpretation was tested by considering the ”failed” sample as a uni-axial test with the peak compression force equal to the set radial compression. It was then possible

to see if it crossed the estimated failure slope of the two other samples and if it failed before the test was started. This seemed appropriate for all configurations of this type. When plotted in this way it could be defined as a type 1) development and these failure slopes were also used for the estimation of cohesion values and friction angles, in total 13 of 20 peak stress configurations were defined as type 1).

Cohesion and internal friction angles have been calculated from estimated failure slopes of the peak shear stress – confinement developments and the residual shear stress – confinement developments. The results are presented in Tables 1 and 2 for the peak stresses and residual stresses accordingly. The configurations laying well above or below two times the standard deviation and the configurations giving negative cohesion values were excluded.

Table 1. Cohesion and friction angles for peak stress

	n	Mean cohesion (c)	SD c_{SD}	Mean friction angle (ϕ)	SD (ϕ_{SD})
Fresh configurations (all)	5	0.036	±0,017	30.93°	±5.69°
-2.5°C	1	0.028	±0	27.53°	±0°
-8.5°C	4	0.038	±0.019	31.74°	±5.85°
Saline configurations	8	0.028	±0.031	35.85°	±15.32°
-2.5°C	3	0.026	±0.021	33.90°	±15.31°
-8.5°C	5	0.028	±0.036	37.25°	±14.69°

Table 2. Cohesion and friction angles for residual stress

	n	Mean cohesion (c)	SD c_{SD}	Mean friction angle (ϕ)	SD (ϕ_{SD})
Fresh configurations (all)	5	0.007	±0,003	23.47°	±10.54°
-2.5°C	1	0.006	±0.002	23.18°	±8.10°
-8.5°C	4	0.008	±0.006	23.62°	±3.05°
Saline configurations	7	0.009	±0.006	25.03°	±10.00°
-2.5°C	3	0.006	±0.003	25.86°	±11.81°
-8.5°C	4	0.011	±0.006	24.40°	±7.85°

Discussion

Comparing the fresh and saline configurations, the mean cohesion values were found to be 30 % higher for the fresh than the saline samples for the peak shear stresses. For the residual stresses, the cohesion values were all close to zero as expected, but the saline gave somewhat higher values. The mean internal friction angles were higher for the saline configurations for both peak and residual stresses. This indicates that the stresses of the fresh samples were less influenced by increasing confinement.

Comparing the peak and residual stresses, the mean cohesion values were lower for the residual stress and the internal friction value lies in the lower part of the range of the peak stresses. The standard deviations were also found to be smaller for the residual stresses.

This would be expected from the assumption that the residual stress represents friction, which is less dependent on the small deviations between tests and between each sample.

A temperature dependency was also visible from the results. All mean cohesion values were higher for the lower initial temperature. Freeze-bonds have been found to have increasing strength for decreasing temperatures (Shafrova and Høyland, 2008), (Repetto-Llamazares et al., 2011), which would account for this finding. No obvious correlation was found between the cohesion/friction angle and the submersion time. A clear connection between the peak shear stress and the submersion time would be expected to be reflected in the cohesion and internal friction angle, a larger sample basis may give an answer to this.

The cohesion values were in the range 0.003 – 0.099 MPa and the internal friction 0.28 – 0.78 for the peak stresses. For the residual 0.001 – 0.018 MPa and 0.20 – 0.64. Repetto-Llamazares et al. (2011) found cohesion values in the range of 0.0014 – 0.0044 MPa and internal friction values in the range 0.19 - 0.59. Shafrova and Høyland (2008) extrapolated these results and compared them with their own, they fitted well. The results were in the same range as ours even though two different test set-ups were used, but a few configurations gave very high cohesion values in comparison. Schulson and Fortt (2012) found friction values in the range from 0.15 to 0.19 and cohesions from 0.0032 to 0.0056 MPa for sliding velocity of 1 mm/s and T_i = -10°C. The friction coefficients fits with the lower range of our residual friction angles, and their cohesions are somewhat less than what we found, but still close to zero.

CONCLUSIONS

The freeze-bond stresses were found to be in the same range for the uni-axial samples as found for previous experiments. The freeze-bond stress dependency of submersion time, initial temperature and salinity was all found to reinforce the existing theory. This gave a good basis for studying the effect of radial confinement.

Both our results and results from earlier similar set-ups (sample loaded 45° to the freeze-bond orientation) gave higher peak shear stresses than direct shear experiments. This can be explained by the introduction of Mohr-Coulombs failure criterion. We found values in the range 0.003 – 0.099 MPa for cohesion and 16 – 45° (0.28 - 0.78rad) for internal friction for the peak stresses. For the residual stresses the cohesion values were approaching zero and internal friction angles were in the range 11 – 37° (0.19 - 0.65rad). The estimated cohesion and friction values were in the same range and in agreement with earlier measurements, no clear difference was found between the direct shear tests and the tests with a set-up angle.

Comparing the fresh with the saline configurations the mean cohesion values were found to be 30 % higher. The mean internal friction angles were higher for the saline configurations. A dependency on initial temperature was also seen by the cohesion values, higher cohesion for the lower initial temperature of -8.5°C.

The fresh ice had only strong enough freeze-bonds for short submersion times at the initial temperature of -2.5°C. How the freeze-bonds disintegrates we do not know.

ACKNOWLEDGEMENT

We wish to acknowledge Aleksey Shestov and Jomar Finseth for their contributions to conducting the experiments. We also wish to acknowledge the support from the Research Council of Norway through the Center for Research-based Innovation SAMCoT and the support from all SAMCoT partners.

REFERENCES

Ettema, R., Schaefer, J., 1986. Experiments on freeze-bonding between ice blocks in floating ice rubble. Journal of Glaciology 32 (112), 397–403.

Helgøy, H., Skog Astrup, O., Høyland, K. V., 2013. Laboratory work on freeze-bonds in ice rubble, part 1: Experimental set-up, ice-properties and freeze-bond texture. Port and Ocean Engineering under Arctic Conditions.

Høyland, K. V., Møllegaard, A., 2014. Mechanical behaviour of laboratory made freeze-bonds as a function of submersion time, initial ice temperature and sample size. 22nd IAHR International Symposium on Ice.

Møllegaard, A., 2012. Experimental study on freeze-bonds in laboratory made saline ice.

Repetto-Llamazares, A. H., Høyland, K. V., 2011. Review in experimental studies on freeze-bonds. In: Proceedings of the International Conference on Port and Ocean Engineering Under Arctic Conditions. No. POAC11-021.

Repetto-Llamazares, A. H., Høyland, K. V., Evers, K.-U., 2011. Experimental studies on shear failure of freeze-bonds in saline ice: Part I. Set-up, failure mode and freeze-bond strength. Cold Regions Science and Technology 65 (3), 286–297.

Schulson, E. M., Fortt, A. L., 2012. Friction of ice on ice. Journal of Geophysical Research: Solid Earth 117 (B12).
URL http://dx.doi.org/10.1029/2012JB009219

Shafrova, S., Høyland, K. V., 2008. The freeze-bond strength in first-year ice ridges. small-scale field and laboratory experiments. Cold Regions Science and Technology 54 (1), 54–71.

Shestov, A., Marchenko, A., 2013. Thermodynamic consolidation of ice ridge keels in water at varying freezing points. Norwegian University of Science and Technology.

Appendix

Freeze-bond shear strength calculation

$$A_{ellips} = \sqrt{2}\pi r^2 \tag{4}$$

$$A_{circ} = \pi r^2 \tag{5}$$

$$h = \frac{2r}{\pi}\theta \tag{6}$$

$$\sigma_z = \frac{Measuredpistonforce}{A_{circ}} \tag{7}$$

Force from σ_r in x-direction:

$$\begin{aligned} F &= -2\int_0^{\pi} \sigma_r h(\theta) r cos(\theta) d\theta \\ &= -2\sigma_r \frac{2r}{\pi} r \int_0^{\pi} \theta cos(\theta) d\theta \\ &= -K[\pi * 0 + cos\pi - (0 * 0 + cos0)] \\ &= -K[+(-1) - (1) = 2K \\ &= 8\sigma_r \frac{r^2}{\pi} \end{aligned} \tag{8}$$

Sum of forces in z-direction:
$\sum F_z = 0$

$$\begin{aligned} \sigma_z \pi r^2 - \frac{\sqrt{2}}{2}\tau_{FB}\sqrt{2}\pi r^2 - \sigma_{FB}\frac{\sqrt{2}}{2}\sqrt{2}\pi r^2 = 0 \\ \sigma_z - \tau_{FB}\sigma_{FB} = 0 \\ \tau_{FB} = \sigma_z - \sigma_{FB} \end{aligned} \tag{9}$$

Sum of forces in x-direction:
$\sum F_x = 0$

$$\begin{aligned} 8\sigma_r \frac{r^2}{\pi} + \frac{\sqrt{2}}{2}\tau_{FB}\sqrt{2}\pi r^2 - \frac{\sqrt{2}}{2}\sigma_{FB}\sqrt{2}\pi r^2 = 0 \\ \frac{8}{\pi}\sigma_r + \pi\tau_{FB} - \pi\sigma_{FB} = 0 \\ \sigma_{FB} = \frac{8}{\pi^2}\sigma_r + \tau_{FB} \end{aligned} \tag{10}$$

Equation 9 in equation 10

$$\begin{aligned}\sigma_{FB} &= \frac{8}{\pi^2}\sigma_r + \sigma_z - \sigma_{FB} \\ &= \frac{4}{\pi^2}\sigma_r + \frac{1}{2}\sigma_z \\ \tau_{FB} &= \sigma_z - \frac{4}{\pi^2}\sigma_r - \frac{1}{2}\sigma_z \\ &= \frac{1}{2}\sigma_z - \frac{4}{\pi^2}\sigma_r\end{aligned} \tag{11}$$